Macroscopic Fundamental Diagrams for Low-Altitude Air City Transport

Yazan Safadi[1], Rao Fu[2], Quan Quan[2], and Jack Haddad[1]

[1] Technion–Israel Institute of Technology, Faculty of Civil and Environmental Engineering, Technion Sustainable Mobility and Robust Transportation (T-SMART) Laboratory
[2] Beihang University, The School of Automation Science and Electrical Engineering

SHORT SUMMARY

Low-altitude aircraft is being developed as a new mode of urban transport; consequently, the penetration of low-altitude passenger and delivery aircraft into the urban airspace is inevitable soon. This will give rise to new urban air transport systems, called low-altitude air city transport (LAAT) systems.

Inspired by urban road networks, this paper investigates the collective and aggregate aircraft traffic flow diagrams, i.e. Macroscopic Fundamental Diagrams (MFDs) for LAAT systems. Firstly, aircraft collision-avoidance models with cooperative distributed control algorithms from the literature are implemented to describe the low-altitude aircraft interactions, implying the microscopic traffic behavior. Afterwards, using the generalized definitions of Edie, the MFD is constructed for LAAT networks, by linking flow, density, and speed. Different case study examples are simulated to analyze the MFD shapes for LAAT systems, considering different microscopic collision avoidance approaches and the effects of aircraft and airspace settings.

Keywords: Traffic Flow Theory, Macroscopic Fundamental Diagram, Low-Altitude Air City Transport System.

1. INTRODUCTION

The Wright brothers made a significant impact on the evolution of aviation more than a century ago when they invented the airplane. In recent years, modern advances in aviation and communication technologies have pushed the sphere of urban air mobility (UAM) considerably. A new mode of urban air transport, the low altitude passenger and delivery aircraft, has been developed and will inevitably penetrate the urban airspace. It will lead to new urban air transport systems, namely low-altitude air city transport (LAAT). Such systems will include aircraft operated with or without pilots, transferring passengers and goods in urban areas. As a result, we will enter the new era of urban air mobility.

Similar to roads, growing numbers of passenger and delivery aircraft will cause urban air traffic congestion, and present new air traffic control challenges. To tackle these challenges, one needs to develop traffic management and control strategies to avoid congestion. Accordingly, traffic flow models are needed to develop traffic management and control strategies. Greenshield (Greenshields, Thompson, Dickinson, & Swinton, 1934) was one of the first researchers to establish traffic flow models that relate flow, density, and speed on urban roads. Currently, air traffic management schemes do not take into account traffic flow models. Developing such models would lead to optimal management of airspace.

The literature shows that the Macroscopic Fundamental Diagram (MFD) is a powerful concept for understanding and managing vehicular networks from a theoretical as well as an application-oriented perspective. The concept of MFD was firstly introduced in (Godfrey, 1969), and the empirical verification of its existence with dynamic features was shown in (Geroliminis & Daganzo, 2008). The MFD aggregates the fundamental diagram for the whole network and states traffic variables that inform us of the network condition (free flow or congestion). The MFD is a concave, low-scatter relationship between density K [veh/km] and flow Q [veh/hr], or accumulation N [veh] and production P [veh$\cdot$km/hr]. The MFD concept was also applied to pedestrian flows (Hoogendoorn, Campanella, & Daamen, 2011; Saberi & Mahmassani, 2014; Hoogendoorn, Daamen, Knoop, Steenbakkers, & Sarvi, 2018) by using the generalized definitions of Edie (Edie, 1963) to calculate the MFD variables for 2D motion.

For LAAT systems, there has been very limited exploration of the idea of using traffic flow models in the literature (Jang, Ippolito, Sankararaman, & Stepanyan, 2017; Battista & Ni, 2017; Bulusu, Sengupta, Mueller, & Xue, 2018; Gharibi, Boutaba, & Waslander, 2019; Ivan Tereshchenko & Zou, 2020; Zhou, Jin, Wang, & Sun, 2020; Cummings & Mahmassani, 2021; Haddad, Mirkin, & Assor, 2021). These works introduce elementary traffic flow-oriented models focusing on microscopic or macroscopic levels.

For modeling aircraft dynamics at the microscopic level, it is necessary to determine how the aircraft avoid colliding with each other. In this concern, these studies used different motion control methods to avoid collision between aircraft, e.g. separation assurance by controlling the aircraft-following dynamics (Jang et al., 2017; Battista & Ni, 2017; Gharibi et al., 2019), artificial potential field (APF) (Bulusu et al., 2018), modified voltage-potential algorithms (Ivan Tereshchenko & Zou, 2020), and linear programming based optimization (Cummings & Mahmassani, 2021) or mixed integer linear programming based optimization (Haddad et al., 2021).

To investigate the different approaches, these studies analyzed different traffic characteristics, e.g. speed, separation, number of conflicts, throughput, occupancy, density, flow and capacity. The studies in (Battista & Ni, 2017; Ivan Tereshchenko & Zou, 2020; Cummings & Mahmassani, 2021) showed a similar behavior of MFD shape to ground traffic, however, only the free flow conditions are presented and no system gridlock appears. In (Jang et al., 2017; Haddad et al., 2021), congested regimes are shown in the MFD.

Additionally, some studies investigate the future airspace structure. In (Jang et al., 2017; Battista & Ni, 2017; Gharibi et al., 2019; Zhou et al., 2020; Quan, Li, & Fu, 2021) the airspace structure consists airways and/or intersections, on the other hand, in (Bulusu et al., 2018; Ivan Tereshchenko & Zou, 2020; Cummings & Mahmassani, 2021) an unstructured airspace is considered. In (Haddad et al., 2021), the airspace is divided into several vertical latitudes and each latitude is divided into different regions, where each region may be unstructured or structured.

The current paper aims at deriving and analyzing the aggregate aircraft traffic flow diagrams, i.e. the Macroscopic Fundamental Diagrams (MFDs), which relate the network production and accumulation (or flow and density) for LAAT systems.

2. METHODOLOGY

Future LAAT networks should be efficiently managed by controlling the aircraft flows in the urban airspace. Our goal in the future is to utilize an MFD-based control approach for developing control strategies for LAAT networks, i.e. controlling macroscopically aircraft traffic flows. However, one first needs to implement a microscopic traffic flow model that can describe individual aircraft movement, including travel behavior and its interactions with other aircraft and/or obstacles in the airspace environment. Then, based on the microscopic model one can develop an aggregate model that can capture the traffic network behavior (Haddad et al., 2021).

In this paper, the first step is to build a realistic plant model to capture the airspace dynamics. While in-vehicle ground traffic, the microscopic models focus on the car following and lane changing dynamics, in LAAT systems the microscopic traffic models will mainly focus on conflict detection, separation assurance and new physical dynamics.

There are three main parts in microscopic models: (1) aircraft dynamics, (2) aircraft route, and (3) collision avoidance, as shown in Fig. 1. The aircraft dynamics are usually formed according to kinematic behavior where the states are position $p_i(t)$, velocity $v_i(t)$, and acceleration $a_i(t)$ for an aircraft i with a 3D motion. Maximum velocity $v_{i,m}$ and acceleration $a_{i,m}$ bounds are set for each aircraft. The aircraft route determines individual aircraft routes, where each aircraft departs at a predefined time $t_{i,\text{dep}}$ from a predefined origin point O_i to a predefined destination point D_i. Usually, a direct line between the two points is set as the original route $\tilde{p}_{i,D}(t)$. It is important to note that the final route depends on the collision avoidance algorithm, which should be set. A collision avoidance algorithm should control the aircraft to avoid collisions with other aircraft or obstacles. Several proposed algorithms in (Quan, Fu, & Cai, 2021; Quan, Fu, Li, et al., 2021; Xue & Do, 2019; Soria, Schiano, & Floreano, 2021; Albaba, Musavi, & Yildiz, 2021) can be suitable as well to LAAT systems.

In the following, we follow the developed microscopic model in (Quan, Fu, & Cai, 2021; Quan, Fu, Li, et al., 2021), which can capture the dynamics of the aircraft while maintaining collision-free fly. The proposed collision avoidance algorithms in (Quan, Fu, & Cai, 2021) and (Quan, Fu, Li, et al., 2021) are tested where the aircraft avoids a collision with a predefined safety radius r_s and avoidance radius r_a, by determining the aircraft control input v_c using an Artificial Potential Field (APF) approach based on Lyanpunv-Like functions. In (Quan, Fu, & Cai, 2021), the aircraft objective is to follow predefined waypoints and avoid collision with moving obstacles, in our work we adapt the presented theory to guarantee that the aircraft does not collide with other aircraft. Additionally, another approach (Quan, Fu, Li, et al., 2021) is tested, where the aircraft objective is to follow destination lines instead of waypoints.

Based on this microscopic model, the second step will be to construct the MFD for LAAT networks to capture the network dynamics at the macroscopic level. In this paper, we adopt the spatial structure that divides the airspace into several vertical latitudes and each latitude into different regions, see (Haddad et al., 2021). The MFD can be evaluated per region or for the whole network, where the borders of each region need to be determined. Following the same concept applied to pedestrian flows in e.g. (Hoogendoorn et al., 2018), the main traffic characteristics and physics laws of vehicular traffic flow theory can be generalized to aircraft traffic flow by adapting the one-spatial-dimensional flow to two-spatial-dimensional flow or three-spatial-dimensional flow. In the following, the main macroscopic traffic flow variables, i.e. flow, density, speed, production and accumulation are estimated for aircraft flows. We

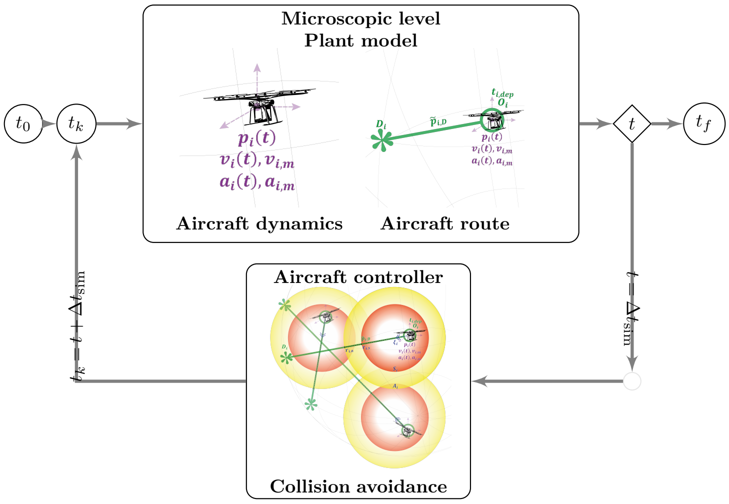

Figure 1: Plant microscopic model

follow the generalized definitions of Edie (Edie, 1963) to calculate the MFD variables, given in e.g. (Hoogendoorn et al., 2011; Saberi & Mahmassani, 2014) for pedestrian flows.

To capture the microscopic and macroscopic levels of aircraft traffic flow, the last step is to simulate LAAT systems based on the dynamic aircraft model and distributed controller. The goal is to utilize the LAAT flow simulation to aggregately derive and investigate MFDs for LAAT networks. A general description of the simulation structure is shown in Fig. 2. To set up a simulation run, one has to determine the simulation inputs, which include: airspace network, aircraft setting, and traffic and simulation settings. These inputs are fed to the aircraft dynamics and traffic flow models, and the collision-avoidance controller. It is possible to conduct a wide range of analyses and studies of the model's outputs, but in this study our main interest is the aircraft trajectories. The aircraft trajectories are used to construct the MFD variable (flow Q, density K, speed U, production P and accumulation N). In the following, we focus on describing the inputs.

The airspace network defines the flight's area and rules, similar to ground traffic networks where the roads and nodes (intersections or roundabouts) are defined. Airspace network components include the geometry of the area, flight routes, and airspace structure. In this paper, we follow the airspace structure presented in (Haddad et al., 2021). Hence, the airspace network here is: (i) a 2D network where flight is allowed on the X-Y plane, with no change in the altitude, (ii) there is no structure of flight routes so that the aircraft can fly in any direction inside the network, i.e. there are neither airways nor intersections in the network. Different network area values are tested to analyze the effect on the simulation results.

The aircraft setting determines the properties and parameters for the aircraft dynamics. In the simulation results of this study, the maximum speed v_{m} is chosen as 20 [m/s] and the maximum acceleration a_{m} is chosen as 5 [m/s^2]. Moreover, the collision avoidance method in (Quan, Fu, & Cai, 2021; Quan, Fu, Li, et al., 2021) determines three spaces around each aircraft to actuate the distributed controller, i.e safety, avoidance, and detection. In this study, the following values are chosen: the safety radius r_{s} is 15 [m], the avoidance radius r_{a} is 22.5 [m] ($r_{\mathrm{a}} = 1.5 \cdot r_{\mathrm{s}}$), and the detection radius r_{d} is 45.5 [m] ($r_{\mathrm{d}} = r_{\mathrm{s}} + r_{\mathrm{a}} + 2 \cdot \max \frac{v_{\mathrm{m,i}}}{l_i}$). Later, the impact of the safety

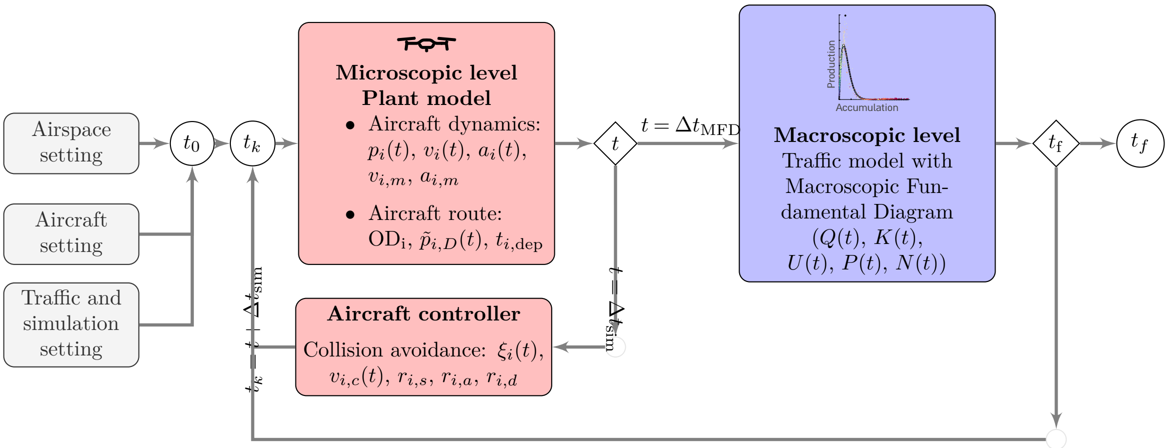

Figure 2: Simulation environment setup that combines the microscopic and macroscopic levels of LAAT systems

radius value and the maximum velocity on the simulation results is analyzed.

Last, similar to ground traffic simulation, traffic and simulation settings are defined as follows: (i) the simulation duration t_f is set to 1.5 [hr] (5400 [s]); (ii) the simulation time step Δt_{sim} is set to 0.5 [s] (note that the maximum value is $\Delta t_{\mathrm{sim}} < r_\mathrm{a}/v_\mathrm{m}$); (iii) the traffic inflow $Q_{\mathrm{in}}(t)$ [aircraft/s] describes the number of aircraft entering the network at time t. The maximum traffic inflow value $Q_{\mathrm{in,max}}$ is set for each scenario, and then the traffic inflow profile is divided into 3 periods of 0.5 [hr], in the first and last period, i.e. 0.0 [hr] $\leq t < 0.5$ [hr] and 1.0 [hr] $\leq t < 1.5$ [hr], the traffic inflow is equal to $Q_{\mathrm{in}} = 0.5 \cdot Q_{\mathrm{in,max}}$. During the second period, i.e. 0.5 [hr] $\leq t < 1$ [hr], the traffic inflow is equal to $Q_{\mathrm{in}} = Q_{\mathrm{in,max}}$; and (iv) the origin and destination of each aircraft are randomly defined at the network boundaries.

3. RESULTS AND DISCUSSION

Several case study examples are presented to construct MFD curves for LAAT. The microscopic traffic model of each LAAT aircraft is based on the models presented in (Quan, Fu, & Cai, 2021; Quan, Fu, Li, et al., 2021). Based on the simulated data results, the MFD is constructed by using the Generalized Edie's definitions (Edie, 1963) to estimate the MFD variables.

The case study examples examine the following issues: constructing an MFD, the effect of the airspace network size, and the effect of the aircraft safety radius. Additionally, the effect of heterogeneous traffic is considered, where a random variety in the aircraft safety radius and maximum speed values are set. Each case study example is evaluated from several simulation scenarios. Furthermore, another microscopic model is examined, where the aircraft objective is to follow destination lines (Quan, Fu, Li, et al., 2021) instead of waypoints (Quan, Fu, & Cai, 2021). In this paper, we present only the MFD results to compare between the two models.

The following is the simulation results with the microscopic models and the simulation setup according to the description in Section 2. The network area is set to 0.5 [km] by 0.5 [km], the aircraft safety radius is $r_s = 15$ [m], and the maximum velocity is $v_m = 20$ [m/s]. The full shape of the MFD is extracted from different scenarios, as each scenario has a different maximum inflow rate in the aircraft inflow profile, where the maximum inflow rate value varies from 360 [aircraft/hr] to 4320 [aircraft/hr] (0.1 [aircraft/s] to 1.2 [aircraft/s]). The MFD variables are calculated in a specific time period $\Delta t_{\text{MFD}} = 60$ [s], i.e. each point on the MFD is an aggregated value of 60 [s] of simulated data.

The MFD results for LAAT flow operation, relating aircraft flow, density and speed in urban airspace, are shown in Fig. 3. The MFD curves for the LAAT network resemble those observed for ground traffic networks. As can be seen in the figures, the scatter of the flow grows as traffic density increases. Nonetheless, the average speed is a decreasing function of traffic density. Similarly, the flow is a concave unimodal function of density. The peak of this function corresponds to the theoretical capacity of the system.

Based on the MFD concept, we verified in our results that as the density increases, the traffic flow increases as well up to a peak flow. This regime is the uncongested regime, where beyond that regime the congested regime starts as the traffic becomes congested and flow decreases. In the congested regime, the aircraft impede each other, as they slow down and/or deviate from their planned paths to avoid losses of separation. The flow reaches its minimum steady-state value at a maximum aircraft density that maintains safety. In the uncongested part, the results are similar to the results in (Bulusu et al., 2018; Ivan Tereshchenko & Zou, 2020; Cummings & Mahmassani, 2021), although the congested part is different due to the changes in separation algorithm and distances, and the characteristics of the aircraft.

Fig. 3 presents the MFD relationship between flow, density, and speed, while the relationship between production and accumulation is shown in Fig. 4. Two microscopic model approaches were tested, in Fig. 3 (a) and Fig. 4 (a) the waypoints approach results are presented (Quan, Fu, & Cai, 2021); and in Fig. 3 (b) and Fig. 4 (b) the destination lines approach results are presented (Quan, Fu, Li, et al., 2021). As seen from the comparison of (Quan, Fu, & Cai, 2021; Quan, Fu, Li, et al., 2021) in Table. 1, using a destination lines objective instead of a waypoints objective for the aircraft controller increases the maximum production in the network, even though the critical accumulation is slightly smaller. A similar comparison between different settings is presented in Table. 2.

Table 1: Comparison between microscopic models

Objective	$\tilde{N}_{\text{cr}}$ [aircraft]	$\tilde{P}_{\text{max}}$ $\left[\frac{\text{aircraft}\cdot\text{m}}{\text{s}}\right]$	$\tilde{P}(N)$
Waypoints	18.8	113.0	$14.829 \cdot N \cdot e^{\frac{-1}{1.089}\cdot\frac{N}{18.15}^{1.089}}$
Destination lines	16.9	167.3	$25.396 \cdot N \cdot e^{\frac{-1}{1.059}\cdot\frac{N}{16.94}^{1.059}}$

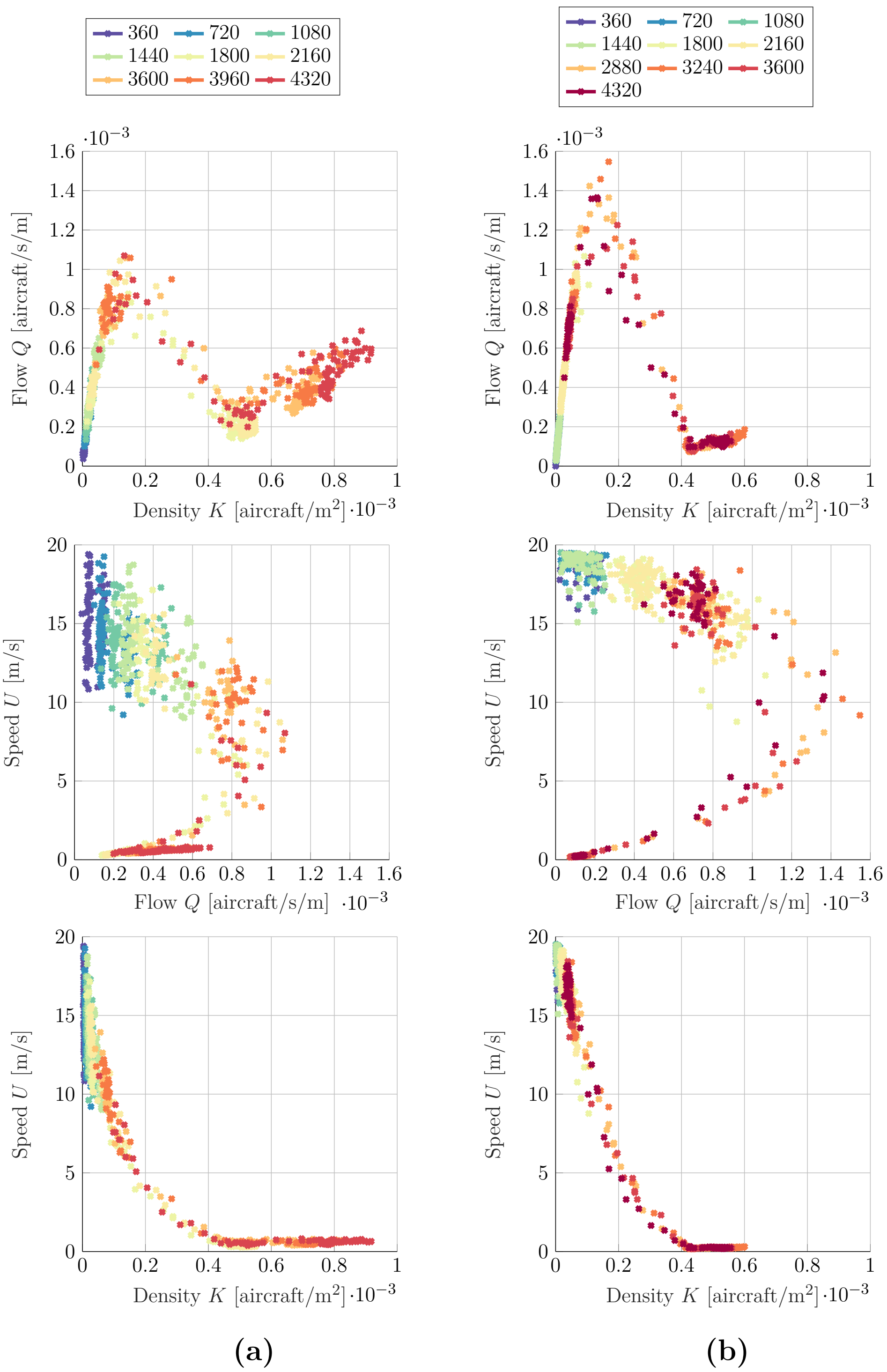

Figure 3: Simulation results for the relationship between flow Q, density K, and speed U: (a) waypoints approach, and (b) destination lines approach.

4. Concluding remarks

The macroscopic fundamental diagram for low altitude air city transport system is presented in this paper. The simulation framework is constructed with a microscopic model that applies

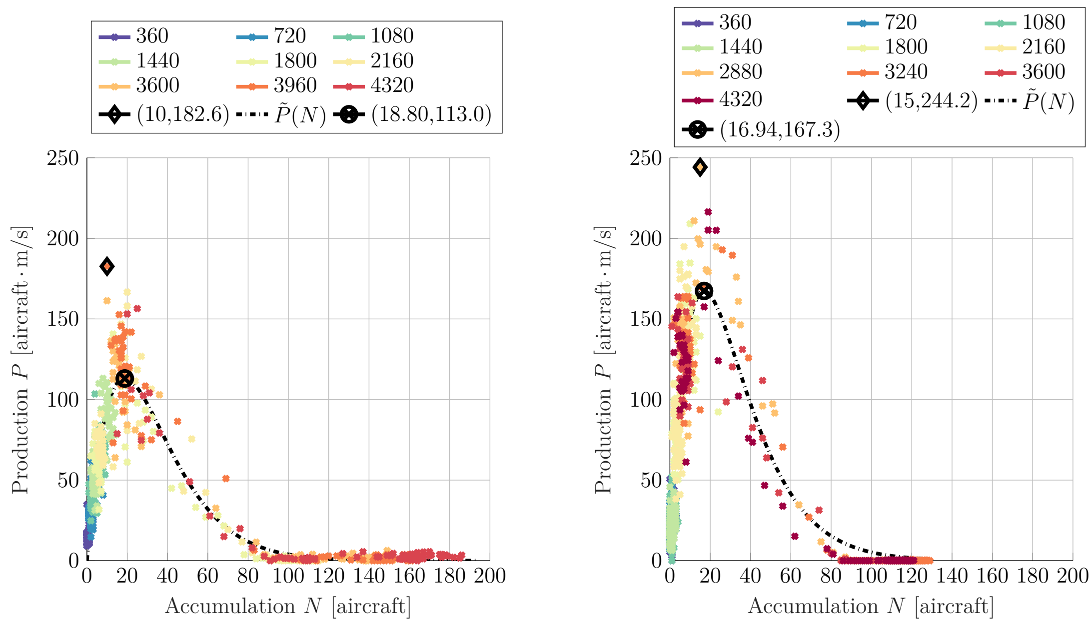

(a) (b)

Figure 4: Simulation results for the relationship between production P and accumulation N: (a) waypoints approach, and (b) destination lines approach.

Table 2: Comparison between different settings

Network	r_s [m]	v_m $[\frac{\text{m}}{\text{s}}]$	$\tilde{N}_{\text{cr}}$ [aircraft]	$\tilde{P}_{\max}$ $[\frac{\text{aircraft}\cdot\text{m}}{\text{s}}]$	$\tilde{P}(N)$
2 [km] X 2 [km]	15	20	205.5	945.1	$8.938 \cdot N \cdot e^{\frac{-1}{1.505}\cdot\frac{N}{205.5}^{1.505}}$
1 [km] X 1 [km]	15	20	58.9	309.9	$11.284 \cdot N \cdot e^{\frac{-1}{1.311}\cdot\frac{N}{58.91}^{1.311}}$
0.5 [km] X 0.5 [km]	15	20	18.8	113.0	$14.829 \cdot N \cdot e^{\frac{-1}{1.089}\cdot\frac{N}{18.15}^{1.089}}$
2 [km] X 2 [km]	10	20	401.8	2022.5	$8.477 \cdot N \cdot e^{\frac{-1}{1.919}\cdot\frac{N}{401.8}^{1.919}}$
2 [km] X 2 [km]	15	20	205.5	945.1	$8.938 \cdot N \cdot e^{\frac{-1}{1.505}\cdot\frac{N}{205.5}^{1.505}}$
2 [km] X 2 [km]	20	20	121.9	568.6	$9.192 \cdot N \cdot e^{\frac{-1}{1.475}\cdot\frac{N}{121.9}^{1.475}}$
0.5 [km] X 0.5 [km]	[10, 20]	20	13.5	121.5	$23.737 \cdot N \cdot e^{\frac{-1}{1.032}\cdot\frac{N}{13.48}^{1.032}}$
0.5 [km] X 0.5 [km]	15	[10, 30]	15.5	106.6	$17.582 \cdot N \cdot e^{\frac{-1}{1.067}\cdot\frac{N}{15.48}^{1.067}}$
0.5 [km] X 0.5 [km]	[10, 20]	[10, 30]	12.3	80.4	$22.858 \cdot N \cdot e^{\frac{-1}{0.798}\cdot\frac{N}{12.31}^{0.798}}$

collision avoidance methods from the literature. The MFD variables are calculated by utilizing the generalized definition of Edie. Two approaches are tested where the aircraft objective is to follow waypoints or destination lines. Several simulation settings are tested, including different sizes, aircraft safety radiuses, and maximum speeds. Moreover, a heterogeneous traffic case is tested in which a variety of aircraft settings are set.

The MFD shape of the LAAT system can be estimated by an exponential function, where the maximum flow point divides it into two conditions, free flow and congestion, similar to the ground traffic flow. The maximum flow value is the airspace capacity. In terms of traffic control, we want to avoid congestion by avoiding reaching the capacity. In conclusion, this research estimates different MFD shapes based on different simulation settings. This contributes to the literature as new control strategies can be developed based on this study.

ACKNOWLEDGMENT

The research presented in this paper was (partially) funded by the Israeli Smart Transportation Research Center (ISTRC) and the EuroTech Alliance.

REFERENCES

Albaba, B. M., Musavi, N., & Yildiz, Y. (2021, dec). A 3d game theoretical framework for the evaluation of unmanned aircraft systems airspace integration concepts. *Transportation Research Part C: Emerging Technologies*, *133*, 103417. doi: 10.1016/j.trc.2021.103417

Battista, A., & Ni, D. (2017, jan). Modeling small unmanned aircraft system traffic flow under external force. *Transportation Research Record: Journal of the Transportation Research Board*, *2626*(1), 74–84. doi: 10.3141/2626-10

Bulusu, V., Sengupta, R., Mueller, E. R., & Xue, M. (2018, jun). A throughput based capacity metric for low-altitude airspace. In *2018 aviation technology, integration, and operations conference.* American Institute of Aeronautics and Astronautics. doi: 10.2514/6.2018-3032

Cummings, C., & Mahmassani, H. (2021, jul). Emergence of 4-d system fundamental diagram in urban air mobility traffic flow. *Transportation Research Record: Journal of the Transportation Research Board*, *2675*(11), 841–850. doi: 10.1177/03611981211020005

Edie, L. (1963). Discussion of traffic stream measurements and definitions. In *Almond, j. (ed.). proceedings of the 2nd international symposium on the theory of traffic flow* (pp. 139–154). OECD, Paris, France.

Geroliminis, N., & Daganzo, C. F. (2008, nov). Existence of urban-scale macroscopic fundamental diagrams: some experimental findings. *Transportation Research Part B*, *42*(9), 759-770. doi: 10.1016/j.trb.2008.02.002

Gharibi, M., Boutaba, R., & Waslander, S. L. (2019). *3d traffic flow model for uavs.*

Godfrey, J. W. (1969). The mechanism of a road network. *Traffic Engineering and Control*, *11*(7), 323–327.

Greenshields, B. D., Thompson, J., Dickinson, H., & Swinton, R. (1934). The photographic method of studying traffic behavior. In *Highway research board proceedings* (Vol. 13).

Haddad, J., Mirkin, B., & Assor, K. (2021, dec). Traffic flow modeling and feedback control for future low-altitude air city transport: An MFD-based approach. *Transportation Research Part C: Emerging Technologies*, *133*, 103380. doi: 10.1016/j.trc.2021.103380

Hoogendoorn, S., Campanella, M., & Daamen, W. (2011). Fundamental diagrams for pedestrian networks. In R. D. Peacock, E. D. Kuligowski, & J. D. Averill (Eds.), *Pedestrian and evacuation dynamics* (pp. 255–264). Boston, MA: Springer US.

Hoogendoorn, S., Daamen, W., Knoop, V., Steenbakkers, J., & Sarvi, M. (2018, sep). Macroscopic fundamental diagram for pedestrian networks: Theory and applications. *Transportation Research Part C: Emerging Technologies*, *94*, 172–184. doi: 10.1016/j.trc.2017.09.003

Ivan Tereshchenko, M. H., & Zou, B. (2020). *Macroscopic fundamental diagram for air traffic: Preliminary theoretic results and simulation findings* (Tech. Rep.).

Jang, D.-S., Ippolito, C. A., Sankararaman, S., & Stepanyan, V. (2017, jan). Concepts of airspace structures and system analysis for UAS traffic flows for urban areas. In *AIAA information systems-AIAA infotech @ aerospace.* American Institute of Aeronautics and Astronautics. doi: 10.2514/6.2017-0449

Quan, Q., Fu, R., & Cai, K.-Y. (2021). Practical control for multicopters to avoid non-cooperative moving obstacles. *IEEE Transactions on Intelligent Transportation Systems*, 1–19. doi: 10.1109/tits.2021.3096558

Quan, Q., Fu, R., Li, M., Wei, D., Gao, Y., & Cai, K.-Y. (2021). Practical distributed control for VTOL UAVs to pass a virtual tube. *IEEE Transactions on Intelligent Vehicles*, 1–1. doi: 10.1109/tiv.2021.3123110

Quan, Q., Li, M., & Fu, R. (2021). Sky highway design for dense traffic. *IFAC-PapersOnLine*, *54*(2), 140–145. doi: 10.1016/j.ifacol.2021.06.019

Saberi, M., & Mahmassani, H. S. (2014, jan). Exploring areawide dynamics of pedestrian crowds. *Transportation Research Record: Journal of the Transportation Research Board*, *2421*(1), 31–40. doi: 10.3141/2421-04

Soria, E., Schiano, F., & Floreano, D. (2021, may). Predictive control of aerial swarms in cluttered environments. *Nature Machine Intelligence*, *3*(6), 545–554. doi: 10.1038/s42256-021-00341-y

Xue, M., & Do, M. (2019, jun). Scenario complexity for unmanned aircraft system traffic. In *Aiaa aviation 2019 forum* (p. 3513). American Institute of Aeronautics and Astronautics. doi: 10.2514/6.2019-3513

Zhou, J., Jin, L., Wang, X., & Sun, D. (2020). Resilient UAV traffic congestion control using fluid queuing models. *IEEE Transactions on Intelligent Transportation Systems*, 1–12. doi: 10.1109/tits.2020.3004406